Characterization of $LaCl_3$:Ce detectors for gamma spectroscopy

A Dissertation
Submitted in partial fulfillment of the requirements for the award of the degree of

Master of Technology in Solid State Electronic Materials

Submitted by

Kalyani (Enroll No: 14550010)

Under the supervision of

Dr. Anil Kumar Gourishetty

DEPARTMENT OF PHYSICS
INDIAN INSTITUTE OF TECHNOLOGY ROORKEE
ROORKEE-247667(INDIA)
MAY 2016

Candidate's Declaration

I hereby declare that the work which is being presented in this Dissertation entitled **"*Characterization of $LaCl_3$:Ce detectors for gamma spectroscopy*"** and submitted in partial fulfillment of the requirements of the degree of **Master of Technology in Solid State Electronic Materials** to the **Department of Physics, Indian Institute of Technology Roorkee** is an authentic record of my own work carried out during the period of July 2015 to May 2016 under the supervision of **Dr. Anil Kumar Gourishetty, Department of Physics, IIT Roorkee.** The matter embodied in this report has not been submitted by me for the award of any other degree in this Institute or any other Institute/University.

(KALYANI)

Date: M. Tech. (SSEM)

Place: Department of Physics

IIT Roorkee

Certification

This is to certify that the dissertation entitled **"*Characterization of $LaCl_3$:Ce detectors for gamma spectroscopy*"** submitted by **Kalyani (Enroll No: 14550010)**, in partial fulfillment for the requirements of the award of degree of **Master of Technology in Solid State Electronic Materials** from IIT Roorkee is a record of her own work carried out under my supervision.

Date: **Dr. Anil Kumar Gourishetty**

Place: Assistant Professor

Department of Physics

IIT Roorkee

ACKNOWLEDGEMENT

I would like to give my deep gratitude to *Dr. Anil Kumar Gourishetty*, Department of Physics IIT Roorkee for his help and guidance throughout this project.

I express my sincere gratitude to my colleague Ms. Nidhi Goel, Ms. Sheetal Rawat and Mrs. Monalisha Dhibar for helped me to carry out the experiments.

Last but not least I give my heartfelt thanks to my friends Mr. Vibhuti Narain Singh, Ms. Rashmi Bhardwaj and Ms. Manisha Sharma who helped me in numerous ways and of course I must extend my cordial thanks towards to my lecturers and administrative staff for their supports during my entire course time.

Finally, warmly I am giving my thanks and deepest gratitude to my family for their supports and encouragements gives throughout my life.

Table of Contents

Chapter 1 Introduction 1

1.1 Scintillation detectors 1

1.1.1 Scintillator 2
1.1.2 Photomultiplier Tube (PMT) 2
1.1.2.1 Photocathode 3

1.1.3 Multichannel Analyser (MCA) 3

1.2 Detector characterisation 3

1.2.1 Energy calibration 3

1.2.2 Energy resolution 4

1.2.3 Time resolution 4

1.2.4 Detection efficiency 5

1.2.4.1 Intrinsic photo-peak efficiency 5

1.2.4.2 Intrinsic total detection efficiency 5

1.2.4.3 Absolute photo-peak efficiency 5

1.2.4.4 Absolute total detection efficiency 5

1.2.5 Coincidence Summing 6

Chapter2 Literature Survey 7

Chapter 3 Theoretical Formalism 11

3.1 Energy resolution 11

3.2 Absolute full energy peak efficiency 12

3.3 Absolute total detection efficiency 12

3.4 Photo-fraction 12

3.5 Coincidence summing 12

3.6 Na-22 13

3.7 Error calculation 14

Chapter 4 Experimental Details 15

4.1 Scintillator detector 16

4.2 Preamplifier 17

4.3 Linear amplifier and CRO 17

4.4 Constant fraction discriminator (CFD) 17

4.5 Delay unit 17

4.6 Time to amplitude converter (TAC) 17

4.7 MCA card 18

4.8 MCA software 19

4.9 Gamma sources 19

Chapter 5 Observations 20

5.1 Energy calibration of $LaCl_3$: Ce 20

5.1.1 Calibration plot 20

5.2 Energy spectra of different sources at different distances 21

5.2.1 Cs-137 21

5.2.2 Zn-65 23

5.2.3 Co-60 24

5.2.4 Na-22 25

Chapter 6 Results and Discussion 27

6.1 Energy resolution at different distances 27

6.2 Timing resolution 28

6.2.1 Speed of light 28

6.3 Efficiencies 29

6.3.1 For single gamma emitters 30

6.3.1.1 Cs-137 30

6.3.1.2 Zn-65 30

6.3.2 Double gamma emitters 31

6.3.2.1 Co-60 31

6.3.2.2 Na-22 31

6.4 Photo-fraction 32

6.4.1 Cs-137 32

6.4.2 Zn-65 32

6.5 Simulations 32

6.5.1 Cs-137 33

6.5.2 Co-60 33

6.5.3 Na-22 34

Chapter 7 Summary 35

Chapter 9 References 37

List of Figures

Figure 1.1 Apparatus with a Scintillating crystal, PMT and data acquisition components 2

Figure 1.2 Experimental arrangements for the $\gamma - \gamma$ coincidence timing measurements 4

Figure 2.1 The comparisons of energy spectra of Cs-137 from $LaCl_3$ and NaI(Tl) 7

Figure 2.2 Energy resolution and intrinsic resolution of $LaCl_3$ and NaI(Tl) 8

Figure 2.3 Total photo-peak efficiency and energy resolution of three $LaCl_3$ (Ce) and coplanar grid CdZnTe detector 8

Figure 2.4 Energy resolution and full energy peak efficiency comparison of $LaCl_3$, LaBr3, NaI(Tl) and CZT detectors 10

Figure 3.1 Representation of Gaussian shape peak with standard deviation σ, the FWHM is given by 2.35σ 11

Figure 4.1 Experimental setup for efficiency and resolution measurements 15

Figure 4.2 Experimental set up for timing measurements 16

Figure 4.3 $LaCl_3$:0.9%Ce scintillatoion detector with operating voltage 0.710kV 16

Figure 4.4 Linear amplifier 17

Figure 4.5 CFD 18

Figure 4.6 TAC 18

Figure 4.7 PCI-express MCA card installed inside PC 18

Figure 4.8 Software interface showing energy spectrum for Cs-137 19

Figure 4.9 Different radioactive gamma sources 19

Figure 5.1 Energy calibration plot using table 4.1 20

Figure 5.2 Energy spectrums for Cs-137 and Na-22 21

Figure 5.3 Energy spectra for Cs-137 for different values of source to detector distance 22

Figure 5.4 Energy spectra for Zn-65 for different values of source to detector distance 24

Figure 5.5 Energy spectra for Co-60 for different values of source to detector distance 25

Figure 5.6 Energy spectra for Zn-65 for different values of source to detector distance 26

Figure 6.1 Resolution vs gamma energy for different values of source to detector separation 27

Figure 6.2 Timing spectra by two $LaCl_3$: Ce operating in coincidence with two 511 photons with energy gating 28

Figure 6.3 Distance vs time graph for $LaCl_3$: Ce 28

Figure 6.4 Variation of absolute photo-peak efficiency of $LaCl_3$: Ce with different values of source to detector distances for 662keV gamma (Cs-137) 29

Figure 6.5 Variation of absolute photo-peak efficiency of $LaCl_3$: Ce with different values of source to detector distances for 1120keV gamma (Zn-65) 30

List of Tables

Table 2.1 Absolute detection efficiency for some new detectors 9

Table 4.1 $LaCl_3$: Ce detector specifications 16

Table 4.2 Gamma sources specifications 19

Table 5.1 Measurement for the calibration of $LaCl_3$ scintillator detector by the point sources Co-60, and Cs-137 20

Table 5.2 Measurement of peak count rates and total counts under spectrum for Cs-137 21

Table 5.3 Measurement of photo- peak count rates and total counts under spectrum for Zn-65 23

Table 5.4 Measurement of photo-peak count rates and sum peak count rate for Co-60 24

Table 5.5 Measurement of photo-peak count rates and sum peak count rate for Na-22 25

Table 6.1 Energy resolution of $LaCl_3$ for different energies 27

Table 6.2 Absolute photo-peak and absolute total detection efficiency at different distances for Cs-137 29

Table 6.3 Absolute photo-peak and absolute total detection efficiency at different distances for Zn-65 30

Table 6.4 Absolute photo-peak and absolute total detection efficiency at different distances for Co-60 31

Table 6.5 Absolute photo-peak and absolute total detection efficiency at different distances for Na-22 31

Table 6.6 Measured photo-fraction of $LaCl_3$:Ce for Cs-137 at different source to detector distance 32

Table 6.7 Measured photo-fraction of $LaCl_3$:Ce for Zn-65 at different source to detector distance 32

Table 6.8 Measured and simulated values of photo- peak efficiencies for Cs-137 at different source to detector distance 33

Table 6.9 Measured and simulated values of photo-peak efficiencies for Co-60 at different source to detector distance 33

Table 6.10 Measured and simulated values of photo-peak efficiencies for Na-22 at different source to detector distance 34

Table 6.11 Measured and simulated values of total detection efficiencies for Na-22 at different source to detector distance 34

Abstract

Cerium (Ce) doped $LaCl_3$ and $LaBr_3$ have been invented by Delft and Bern Universities and some other groups. Their commercial availability has been made by Saint-Gobain. This project aims to characterize $LaCl_3$:Ce scintillator detector for the gamma ray spectrometry. The study includes determination of detection efficiency, energy resolution, time resolution and photo-fraction. $LaCl_3$:Ce detector of the size 25.4 mm × 25.4 mm doped with 0.9% of Ce has good linear response and good energy resolution for gamma rays at room temperature. Timing resolution is also obtained with two $LaCl_3$ detectors operating in coincidence using Na-22 sources that emits 511 keV gammas. The photo-peak efficiency and photo-fraction of 662keV and 1120keV gamma-rays are measured. The absolute photo-peak efficiency and absolute total detection efficiency are measured with Co-60 and corrected for coincidence summing. Also, the measured results are reproduced by GEANT4 simulations assuming detector in a realistic geometry.

Chapter 1

Introduction

The increasing demands of gamma ray detection have paved the way for the development of new inorganic scintillators. Inorganic scintillators are widely used in many applications such as in nuclear and high energy physics, medical imaging, homeland security, environmental monitoring, radioactive isotope verification, national security etc. NaI and CsI are two most commonly used inorganic scintillators in gamma ray spectrometry. A little amount of impurity is added to these crystals to obtain a high light output in visible region. These impurities are called activators. For example Thallium (Tl) acts as an activator in NaI and denoted as NaI(Tl) and activator sodium is added in CsI crystal and denoted as CsI(Na).

Scintillation detectors are the most commonly used radiation detectors. They are widely used in gamma ray as well as neutron detection. When gamma ray interacts with the scintillator crystal it produces fee electrons whose de-excitation results in photon emission. These photons are collected by the PMT to generate an output pulse.

The selection of detector used in these applications is done on the basis of requirements like high efficiency, low dead time, good energy and timing resolution and low cost. Until now there is no single detector which can meet all these requirements. Thus, there has been considerable research and development of new inorganic scintillators with enhanced performance.

$LaCl_3$ doped with Ce, a new inorganic scintillator has been discovered with very attractive scintillation properties. $LaCl_3$:Ce (10%) is highly dense ($3.9 gcm^{-3}$), have light output 46000photons/MeV, high energy resolution 3.2% for 662keV energy, 28ns decay time. Its peak emission wavelength is 350nm. These attractive properties make $LaCl_3$ a very promising crystal in gamma ray spectrometry.

In view of these attractive properties of $LaCl_3$ for gamma ray detection, we have performed investigation of the efficiency, photo-fraction and energy resolution of $LaCl_3$:0.9% Ce crystal with different values of source-detector separation. Timing resolution is also studied for $LaCl_3$ with energy gating. Radiation detectors can be divided into three major groups which are

(1) Gas filled detectors
(2) Semiconductor detector
(3) Scintillation detectors

1.1 Scintillation detectors

Scintillation detectors are the radiation detecting instruments. They are one of the oldest radiation detectors. The measurements can be done with human eye observing the intensity of flashes in the scintillator crystal. The outcome of scintillators is the production of high light output in the visible range. The main advantage of scintillator is that it is highly portable. A PMT is used to collect these photons where a photocathode is used to convert photons into photo-electrons and then a series of

dynodes is used to amplify these photoelectrons and finally an anode is used to collect these photo electrons and produces output signal. The main parts of scintillator detector are

(1) Scintillator
(2) PMT
(3) Electronic system including MCA

1.1.1 Scintillator

The active portion of scintillation detector for radiation detection is a solid/liquid/gas which is called as scintillator. A scintillator produces minute flashes of light when interact with certain radiations. The intensity of light produced by scintillator depends upon the energy of incident radiation. Scintillators based on solid medium can be made in different sizes. The thickness of scintillator determines its ability to absorb and detect radiations. Thin scintillator is the best choice for the detection of high energy beta particles and low energy gamma rays. And, thick scintillator is the best choice for high energy gamma rays.

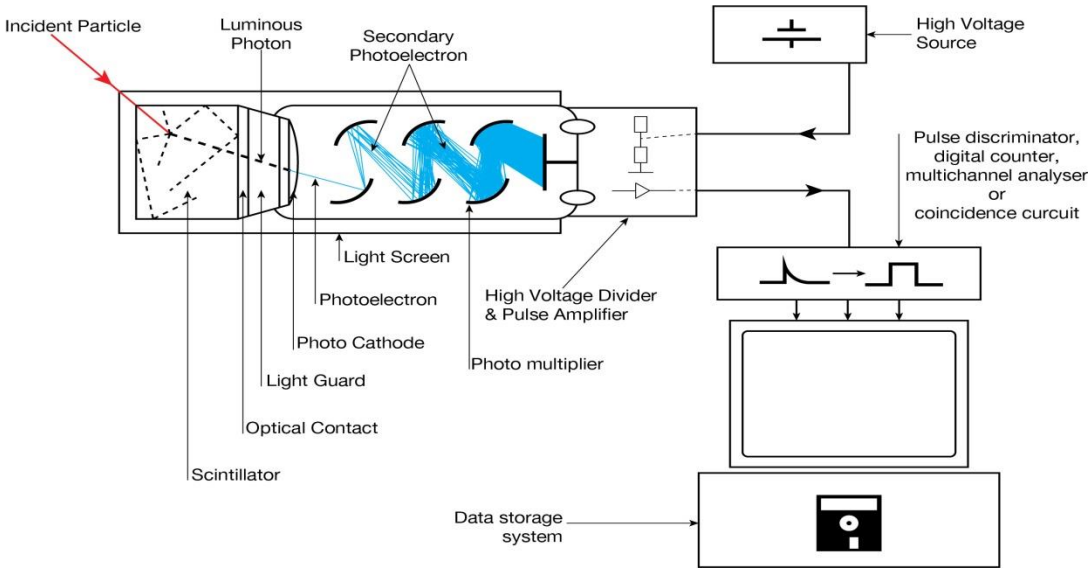

Figure1.1 Apparatus with a scintillating crystal, PMT and data acquisition components

1.1.2 Photomultiplier Tube (PMT)

PMT are the vacuum tubes. Photomultiplier tube is used to convert light signals into electrical signals. A few hundred photons are required to obtain electrical signal. Basic elements of a PMT are a photocathode, dynodes and anode.

1.1.2.1 Photocathode

A photocathode is the first major component in a PMT. It ejects an electron as on when photon interacts with it. The electrons which are ejected by photocathode are called photoelectrons. The photocathode material should be chosen so that it can overcome potential barrier at the surface and the interaction with the material. Typical metal chosen for photocathode possesses 3-4 eV work function and for semiconductors, the work function is 1.5-2 eV.

The sensitivity of photocathode is quoted in terms of quantum efficiency. The quantum efficiency of photocathode is defined as the probability of the conversion of optical photons to an electric signal.

The quantum efficiency of a PMT depends on the wavelength of incident light. There should be resonance in between the spectral response of a photocathode to the emission spectrum of the scintillator.

A PMT also contains a series of dynodes which amplifies the electric signal from photocathode and finally PMT consists of an anode which collects the electron flux and generates output signal.

1.1.3 Multichannel Analyser (MCA)

A multichannel analyser is an apparatus which is used to analyse the input signal that primarily consist of pulses.

1.2 Detector characterisation

(1) Energy calibration
(2) Energy resolution
(3) Detection efficiency
(4) Timing resolution

1.2.1 Energy calibration

The MCA connected to the linear amplifier collects the voltage output and divides it into a number of channels of the same width. In the present work, MCA is used which has 8192 channels. The sensitivity of an analyser depends on the number of channels, more is number of channels more will be the sensitivity.

The sensitivity of an analyser S_{an} is

$$S_{an} = \frac{V_{out}}{N_{Ch}}$$

Where V_{out} is the output signal from amplifier and N_{Ch} is the number channel of the analyser.

Linearity in energy response is the one of the desirable feature of gamma ray detector i.e., height of output signal should be directly proportional to the energy deposited by incident radiation. Energy calibration of the detector is obtained by plotting a graph between peak channel numbers of the full energy peak versus incident radiation energy. Energy calibration is supposed to be done firstly before doing any analysis. Slope of the calibration curve gives the gain of the system.

1.2.2 Energy resolution

Energy resolution of the detector is one of desirable property of the detector. An ideal spectrum of a radioactive source should contain sharp edges and sharp lines but in practice, spectrum obtained from detector has broad peaks and round edges. The energy resolution of detector is the ability to resolve two nearby lying energies so it measures the broadness or width of the photo-peak. So broader peak will corresponds to the low energy resolution of the detector. Energy resolution of the radiation detector depends on the following:

(1) Light output of the detector
(2) Size of the scintillator
(3) Intrinsic resolution of the scintillator
(4) Collection efficiency and quantum efficiency of the PMT

Energy resolution of the detector is obtained by fitting the photo-peak in Gaussian shape. Energy resolution of the scintillation detector generally expressed in percentage. Semiconductor detectors have good energy resolution than scintillation detector due to large number of charge carriers produced which leads to less statistical error.

1.2.3 Time resolution

The time resolution of a scintillation detector gives the ability to define precisely the moment of absorption of a radiation quantum in the detector. Figure 1.2 shows an arrangement for measuring the timing spectrum. In the present work, a double gamma emitter source (Na-22) is placed in between two detectors. The coincidence occurs in between 511 and 1275keV gamma rays.

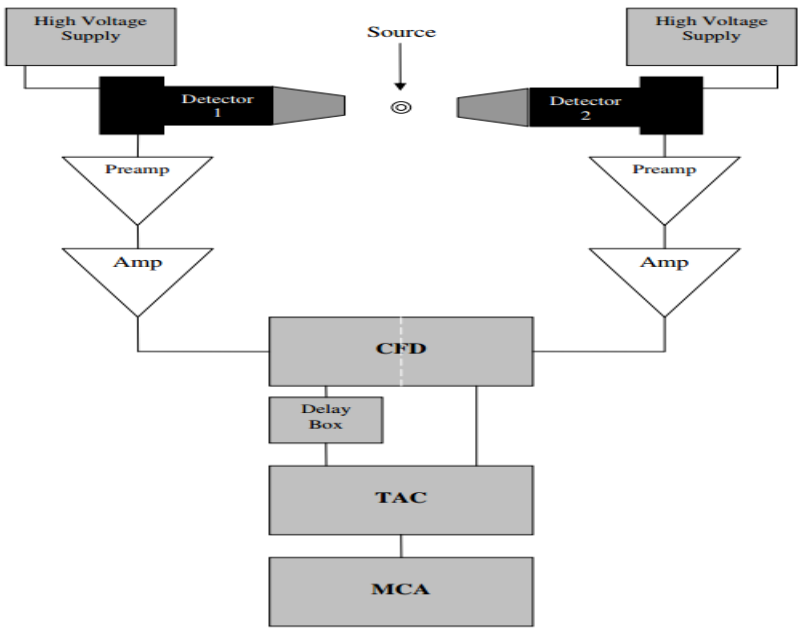

Figure 1.2 Experimental arrangements for the γ-γ coincidence timing measurements

1.2.4 Detection efficiency

It describes the amount of radiation deposited their energy in active part of scintillator. Detection efficiency of a detector depends on following parameters

(1) Incident energy
(2) Shape and size of source and of detector
(3) Measuring geometry

Types of detection efficiencies are:

1.2.4.1 Intrinsic photo peak efficiency

$$\varepsilon_{int,p} = \frac{Number\ of\ counts\ under\ photo\ peak(N_p)}{Number\ of\ radiation\ quanta\ falling\ on\ detector\ surface}$$

1.2.4.2 Intrinsic total detection efficiency

$$\varepsilon_{int,d} = \frac{Number\ of\ pulses\ recorded(N_T)}{Number\ of\ radiation\ quanta\ incident\ on\ the\ detector\ surface N_{\gamma\gamma}}$$

1.2.4.3 Absolute photo peak efficiency

. $$\varepsilon_{abs,p} = \frac{Number\ of\ counts\ under\ photopeak(N_p)}{Number\ of\ radiation\ quanta\ emitted\ by\ source\ in\ all\ directions(A)}$$

1.2.4.4 Absolute total detection Efficiency

$$\varepsilon_{abs,t} = = \frac{Total\ counts\ under\ spectrum(N_T)}{Activity\ of\ the\ source(A)}$$

Number of radiation quanta of energy E which fall on detector can be calculated by using following formula

$$N_{\gamma\gamma} = DI_{\gamma}(E_{\gamma})\Omega/4\pi$$

and number of radiation quanta emitted by source can be obtained by formula

$$A = DI_{\gamma}(E_{\gamma})$$

Where Ω is the solid angle subtended by the detector at the source position, D is the disintegration rate of the source, $I_{\gamma}(E_{\gamma})$ is the fractional number of photons corresponding to energy E_{γ} emitted per disintegration and N_T is total counts under spectrum.

1.2.5 Coincidence summing

When two or more photons simultaneously deposit their energy into the active part of the detector in a time less than the resolving time of detector then true coincidence occurs. In such cases detector is not able to differentiate them so it produces a signal which is the sum of both photon energies. So, we obtain an additional peak in the energy spectrum which is called sum peak. Due to sum peak there is loss in the counts of individual peaks. Thus, to estimate the absolute full-energy absorption efficiency and the absolute total detection efficiency of a detector accurately, a correction to this coincidence summing is required.

Chapter 2

Literature Survey

Guillot-Noel *et al.* [1] presented the optical and scintillation properties of $LuBr_3$: 0.021%, 0.46%, 0.76% Ce, $LaCl_3$:0.57%Ce and $LuCl_3$:0.45%Ce under X-ray and gamma ray excitation. They obtained highest yield 40000± 4000ph/MeV for $LaCl_3$ and an energy resolution 7.0±0.5% for 662 keV gamma.

Van Loef *et al.* [2] investigated $LaCl_3$:10%Ce and obtained Ce^{3+} emission peak at 330nm and 352nm under optical and gamma ray excitation. An energy resolution 3.3±0.3% was observed for 662kev gamma.

As different concentration of Ce doping leads to different light output, energy resolution and different results. Van Loef *et al*. [3] worked on $LaCl_3$ doped with different concentrations of Ce. They investigated $LaCl_3$ doped with 2%, 4%, 10%, 30% Ce and obtained an energy resolution of 3.5± 0.4%, 3.5± 0.4%, 3.1± 0.3%, 3.3 ±0.3%, and 3.4 ±0.3% for 662keV gamma respectively.

Allier *et al.* [4] coupled $LaCl_3$:10%Ce with an 16mm diameter avalanche photodiode instead of PMT and measured an energy resolution 3.7% (FWHM) for 662keV and light output of 46000±5000 ph/MeV. As in many applications APD is used instead of PMT due to its internal gain, high visible photon detection efficiency, fast timing.

Shah *et al.* [5] worked on $LaCl_3$:10%Ce scintillator for gamma ray detection and obtained high light output of 46000ph/MeV, high energy resolution 3.2% (FWHM) for 662keV at room temperature, high timing resolution 264ps (FWHM) have been obtained with $LaCl_3$-PMT and BaF_2-PMT detectors operating in coincidence using Na-22 source(511keV) positron annihilation gamma-ray pair. Scintillation properties, crystal growth and variation of these properties with Ce concentration also reported.

Vidmar *et al*. [6] have proposed a method for correcting the coincidence summing in HPGe detector and reported absolute total detection and photo-peak efficiencies by using double gamma emitters ^{60}Co, ^{46}Sc, ^{94}Nb under the close geometry.

Marcin Balcerzyk *et al*. [7] made a comparison in between $LaCl_3$:10%Ce of 25mm×25 mm and NaI(Tl) of 25×31 mm and obtained following results

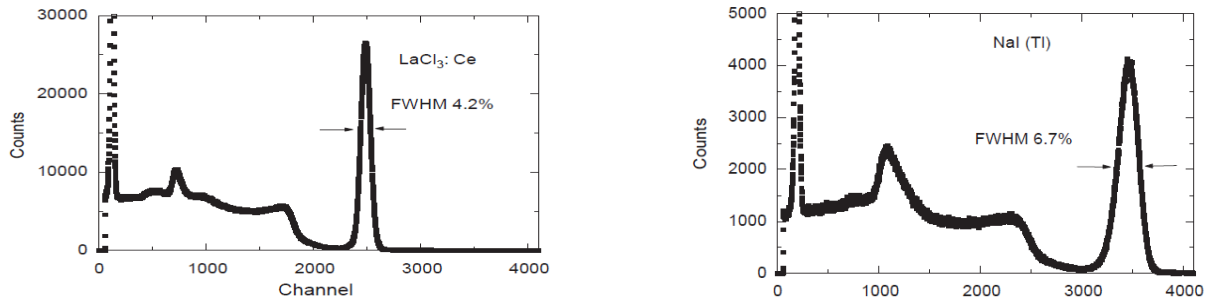

Figure 2.1 The comparison of energy spectra of Cs-137 from $LaCl_3$ and NaI

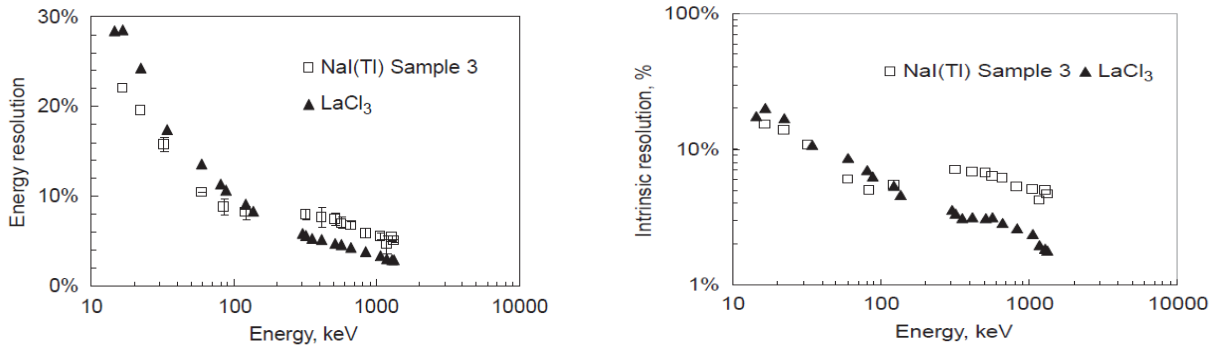

Figure 2.2 Energy resolution and intrinsic resolution of $LaCl_3$ and NaI(Tl)

From above comparisons we can easily conclude that $LaCl_3$ has better energy resolution than NaI(Tl) and $LaCl_3$ showed better intrinsic resolution at higher energies than NaI(Tl).

Mohini W.Rawool-Sullivan *et al.* [8] worked on gamma ray spectroscopy using $LaCl_3$ scintillation detector for use in hand held gamma ray spectrometers. They took $LaCl_3$(Ce) crystals of different sizes and presents energy resolution and total photo-peak efficiency in energy range up to 1350keV at a source detector distance of 25cm. Results obtained are as follows

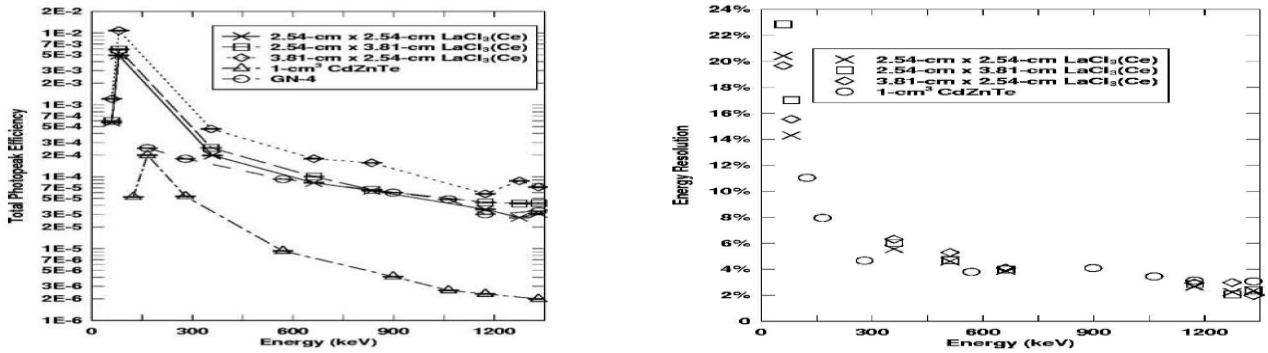

Figure 2.3 Total photo-peak efficiency and energy resolution of three $LaCl_3$(Ce) having different sizes and coplanar grid CdZnTe detector.

From the above results we can easily see that $LaCl_3$ has significant improvement over CdZnTe detectors in most applications due to greater efficiency with comparable energy resolution above 500keV.

Birsan Ayaz-Maierhafer *et al.* [9] presented absolute total and absolute photo-peak efficiencies of NaI:Tl, CdZnTe, HPGe, HPXe, $LaCl_3$:Ce and $LaBr_3$:Ce detectors and were simulated and compared to that of polyvinyl toluene (PVT). The obtained results are as follows:

Table 2.1 ***Absolute detection efficiency for some new detectors***

B. Ayaz-Maierhafer, T.A. DeVol / Nuclear Instruments and Methods in Physics Research A 579 (2007) 410–413

Comparison of the absolute source–detector detection efficiencies of common detectors using a point, line (length = 100 cm) and spherical source (diameter = 15 cm) of ^{60}Co, ^{137}Cs and ^{241}Am at the source-to-detector distance of 25, 100 and 600 cm

Source –detector distance (cm)	Source geometry	Source	Efficiencies	PVT (188.88 cm × 60.96 cm × 5.08 cm)	Relative efficiencies of the detectors									
					PVT (188.88 cm × 60.96 cm × 5.08 cm)	NaI:Tl (7.62 cm diameter × 7.62 cm)	NaI:Tl (10.16 cm × 10.16 cm × 40.64 cm)	NaI:Tl (47 cm × 58.5 cm × 0.95 cm)	NaI:Tl (100 cm diameter × 1 cm)	CdZnTe (1 cm × 1 cm × 1 cm)	HPGe (7.62 cm diameter × 7.62 cm)	HPXe (11.43 cm diameter × 60.96 cm)	$LaBr_3$:Ce (2.54 cm diameter × 2.54 cm)	$LaCl_3$:Ce (5.08 cm diameter × 5.08 cm)
25	Point	^{60}Co	$\varepsilon_{abs,total}$	9.19×10^{-2}	1.0000	0.0379	0.3096	0.3568	0.6835	0.0003	0.0446	0.0303	0.0031	0.0151
			$\varepsilon_{abs,1332\,keV}$	1.13×10^{-4}	1.000	11.88	138.5	53.13	108.0	0.030	11.74	2.856	0.466	3.441
25	Point	^{137}Cs	$\varepsilon_{abs,total}$	1.08×10^{-1}	1.0000	0.0373	0.2933	0.3993	0.7574	0.0003	0.0412	0.0330	0.0032	0.0152
			$\varepsilon_{abs,662\,keV}$	2.23×10^{-4}	1.000	10.66	103.7	69.45	136.7	0.044	9.069	4.203	0.542	3.441
25	Point	^{241}Am	$\varepsilon_{abs,total}$	1.88×10^{-2}	1.0000	0.2591	1.8020	7.6867	11.9325	0.0062	0.2879	0.5455	0.0315	0.1138
			$\varepsilon_{abs,59.5\,keV}$	1.68×10^{-2}	1.000	0.281	1.958	8.353	12.89	0.007	0.311	0.585	0.034	0.123
25	Line	^{60}Co	$\varepsilon_{abs,total}$	8.96×10^{-2}	1.000	0.024	0.2024	0.2719	0.6085	0.0002	0.0288	0.0243	0.0019	0.0095
			$\varepsilon_{abs,1332\,keV}$	1.10×10^{-4}	1.000	7.417	89.97	39.91	94.45	0.017	7.295	2.266	0.275	2.108
25	Line	^{137}Cs	$\varepsilon_{abs,total}$	1.05×10^{-1}	1.0000	0.0238	0.1882	0.2981	0.6628	0.0002	0.0265	0.0266	0.0019	0.0095
			$\varepsilon_{abs,662\,keV}$	2.17×10^{-4}	1.000	6.665	65.75	51.88	119.5	0.025	5.647	3.427	0.324	2.112
25	Line	^{241}Am	$\varepsilon_{abs,total}$	1.84×10^{-2}	1.0000	0.1700	1.1003	5.3072	10.293	0.0040	0.1931	0.4571	0.0224	0.0771
			$\varepsilon_{abs,59.5\,keV}$	1.64×10^{-2}	1.000	0.182	1.187	5.746	11.11	0.004	0.205	0.479	0.024	0.082
25	Sphere	^{60}Co	$\varepsilon_{abs,total}$	4.81×10^{-2}	1.0000	0.0396	0.3073	0.5066	0.9266	0.0004	0.0436	0.0390	0.0036	0.0166
			$\varepsilon_{abs,1332\,keV}$	3.95×10^{-5}	1.000	7.350	86.24	33.19	67.44	0.019	7.357	1.734	0.302	2.177
25	Sphere	^{137}Cs	$\varepsilon_{abs,total}$	5.29×10^{-2}	1.000	0.0391	0.3010	0.4606	0.8599	0.0004	0.0420	0.0366	0.0035	0.0162
			$\varepsilon_{abs,662\,keV}$	6.77×10^{-5}	1.000	10.78	104.8	70.51	138.3	0.045	9.219	4.275	0.557	3.515
100	Point	^{60}Co	$\varepsilon_{abs,total}$	1.77×10^{-2}	1.0000	0.0146	0.1437	0.1876	0.5225	0.0001	0.0168	0.0194	0.0011	0.0056
			$\varepsilon_{abs,1332\,keV}$	2.00×10^{-5}	1.000	4.947	69.57	29.33	85.82	0.010	4.826	2.002	0.174	1.370
100	Line	^{60}Co	$\varepsilon_{abs,total}$	1.74×10^{-2}	1.0000	0.0143	0.1353	0.1808	0.5085	N/A	0.0167	0.0203	0.0010	0.0054
			$\varepsilon_{abs,662\,keV}$	3.19×10^{-5}	1.000	2.925	40.243	17.21	50.80	N/A	2.862	1.282	0.102	0.808
100	Sphere	^{60}Co	$\varepsilon_{abs,total}$	9.36×10^{-3}	1.000	0.0146	0.1381	0.2711	0.7435	0.0001	0.0158	0.0221	0.0012	0.0058
			$\varepsilon_{abs,59.5\,keV}$	6.87×10^{-6}	1.000	3.117	44.02	18.44	54.30	0.006	3.064	1.258	0.1104	0.865
600	Point	^{60}Co	$\varepsilon_{abs,total}$	6.47×10^{-4}	1.0000	0.0117	0.1177	0.1521	0.4538	N/A	0.0134	0.0247	N/A	0.0044
			$\varepsilon_{abs,1332\,keV}$	6.93×10^{-7}	1.000	4.038	58.51	23.99	75.32	N/A	3.945	2.631	N/A	1.109

Alexiev *et al.* [10] presented a comparison of four detectors $LaCl_3$:Ce, NaI(Tl), $LaBr_3$:Ce, CZT for resolution of nuclear material spectra. The energy resolution and full energy peak efficiencies were compared in an energy range 0-1400keV and a source to detector separation of 10cm. Result obtained are as follows

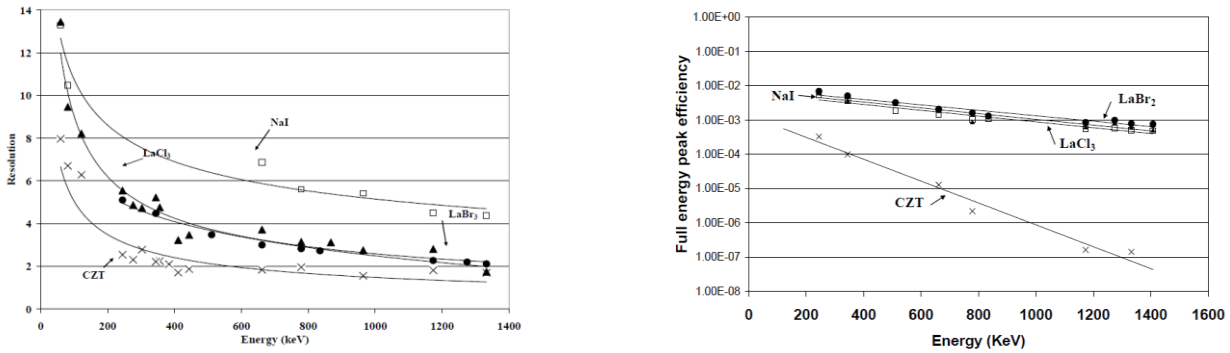

Figure 2.4 Energy resolution and full energy peak efficiency comparison of $LaCl_3$, $LaBr_3$, NaI(Tl) and CZT detectors.

Chapter 3

Theoretical Formalism

3.1 Energy resolution: Energy resolution of the detector is obtained by fitting the photo-peak in Gaussian shape. The Gaussian function can be written as

$$C = \frac{A}{\sigma \times \sqrt{2\pi}} \, exp\left(-\frac{(H-H_0)^2}{2\sigma^2}\right)$$

Where C = number of counts

A = peak area

H_0 = Centroid channel number

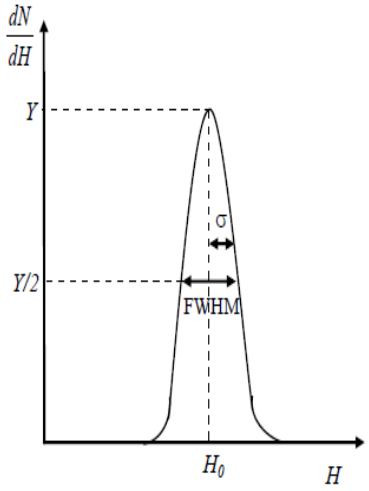

Figure 3.1 Representation of Gaussian shape peak with standard deviation σ, the FWHM is given by 2.35σ.

Energy resolution R of the detector is calculated by using the formula

$$R = \frac{FWHM}{H_0} \times 100$$

Where FWHM = full width at half maximum of photo-peak and H_0 = Centroid channel number

3.2 Absolute full energy peak efficiency

$$\varepsilon_{FEP,abs} = \frac{\text{counts under photopeak } (N_p)}{Number\ of\ radiation\ quanta\ falling\ on\ the\ detector N_{YY}}$$

3.3 Absolute total detection Efficiency

$$\varepsilon_{TDE,abs} = \frac{Total\ counts\ under\ spectrum(N_t)}{Activity\ of\ the\ source(A)}$$

3.4 Photo-fraction

$$\text{PF} = \frac{Counts\ under\ Photopeak}{Total\ Counts\ under\ spectrum}$$

3.5 Coincidence summing correction

For double gamma emitters Vidmar *et al.* [6] presented a method for correcting the coincidence summing in HPGe detectors and reported absolute total detection efficiency and absolute photo-peak efficiency. For Co-60, the transition probability of both gamma rays is almost 100%. The absolute photo peak efficiency of first gamma (E1 < E2) after correcting for coincidence summing can be calculated using an equation

$$\varepsilon_1 = \frac{\varepsilon_{min}+\varepsilon_{max}}{2}$$

Where

$$\varepsilon_{min} = \frac{\left[(N_1-N_2)+((N_1-N_2)^2+4AN_{12})^{1/2}\right]}{2A}$$

And

$$\varepsilon_{max} = \frac{N_1 N_{12}}{AN_2}$$

By knowing the ε_1 value we can easily obtained the other efficiencies by using the following formulas

$$\varepsilon_2 = N_{12}/A\varepsilon_1 \quad (1a)$$

$$\eta_1 = 1 - \varepsilon_1 N_2/N_{12} \quad (1b)$$

$$\eta_2 = 1 - N_1/A\varepsilon_1 \quad (1c)$$

Where N_1 = counts under the photo-peak corresponding to energy E1

N_2 = counts under the photopeak corresponding to energy E2

N_{12} = counts under the sum peak

ε_1 = absolute photo-peak efficiency corresponding to energy E1

ε_2 = absolute photo-peak efficiency corresponding to energy E2

η_1 = absolute total detection efficiency corresponding to energy E1

η_2 = absolute total detection efficiency corresponding to energy E2

A = activity of source

The coincidence-summing correction factors corresponding to the gamma-ray energies E_1 and E_2 have been calculated using the equations

$$C_1=\alpha_1/A\varepsilon_1$$

$$C_2=\alpha_2/A\varepsilon_2$$

3.6 Na-22

Efficiency of $LaCl_3$ for Na-22 is calculated based on the formula derived from *Vidmar et al.* [6] method. Let N_1 and N_2 be the counts rate corresponding to energy E_1 and E_2 respectively when the sum peak is present. N_{12} is the sum peak count rate, A is activity of the gamma source and I_β is positron emission probability.

$$\varepsilon_1 = \left(\frac{\varepsilon_{max}+\varepsilon_{min}}{2}\right)$$

where

$$\varepsilon_{min} = \frac{N_{12}}{2*N_2}\left[\left(\frac{1}{2*I_\beta}-1\right)+\sqrt{\left(\frac{1}{2*I_\beta}-1\right)^2+\frac{4*N_1*N_2}{2*I_\beta*A*N_{12}}}\right]$$

$$\varepsilon_{max} = \left[\frac{(N_1-N_2)+\sqrt{(N_1-N_2)^2+4*A*N_{12}}}{4*I_\beta*A}\right]$$

By knowing $\varepsilon_1$value other efficiencies can be calculated by using following formulas

$$\varepsilon_2 = \frac{N_{12}}{2*I_\beta*A*\varepsilon_1}$$

$$\eta_1 = \frac{1}{2*I_\beta} - \frac{N_2*\varepsilon_1}{N_{12}}$$

$$\eta_1 = 1 - \frac{N_1}{2*I_\beta*A*\varepsilon_1}$$

3.7 Error calculation

The error in calculation of peak efficiency ε_1 as calculated by Vidmar's method is given by

$$\Delta(\varepsilon_1) = \frac{(\varepsilon_{max} - \varepsilon_{min})}{2\sqrt{3}}$$

When α_1 equals α_2, the above expression becomes zero, therefore expanding $\Delta(\varepsilon_1)/\varepsilon_1$ into a series of $(\alpha_1 - \alpha_2)$ up to two terms

$$\frac{\Delta(\varepsilon_1)}{\varepsilon_1} \approx \frac{1}{8*\sqrt{3}}\left(\frac{N_1 - N_2}{N_2}\right)\left(1 - \frac{N_2}{(A*N_{12})^{\frac{1}{2}}}\right) - \frac{1}{16*\sqrt{3}}\left(\frac{N_1 - N_2}{N_2}\right)^2 \qquad (2a)$$

Using eqs.(1), the error in calculation of peak efficiency ε_2 and total efficiencies η_1 and η_2 can be found out by following expressions:

$$\frac{\Delta(\varepsilon_2)}{\varepsilon_2} = \frac{1}{\varepsilon_2}\frac{N_{12}}{A*\varepsilon_1}\frac{\Delta(\varepsilon_1)}{\varepsilon_1} = \frac{\Delta(\varepsilon_1)}{\varepsilon_1} \qquad (2b)$$

$$\frac{\Delta(\eta_1)}{\eta_1} = \frac{1}{\eta_1}\frac{N_2}{N_{12}}\Delta(\varepsilon_1) \approx \frac{1}{\eta_1}\frac{\Delta(\varepsilon_1)}{\varepsilon_1} \qquad (2c)$$

$$\frac{\Delta(\eta_2)}{\eta_2} = \frac{1}{\eta_2}\frac{N_1}{A*\varepsilon_1}\frac{\Delta(\varepsilon_1)}{\varepsilon_1} \approx \frac{1}{\eta_2}\frac{\Delta(\varepsilon_1)}{\varepsilon_1} \qquad (2d)$$

Chapter 4

Experimental Details

The experimental setup consists of following things

(1) Scintillation detector
(2) Pre-amplifier
(3) Linear amplifier
(4) CFD
(5) Delay unit
(6) TAC
(7) CRO
(8) MCA card and software
(9) Gamma sources

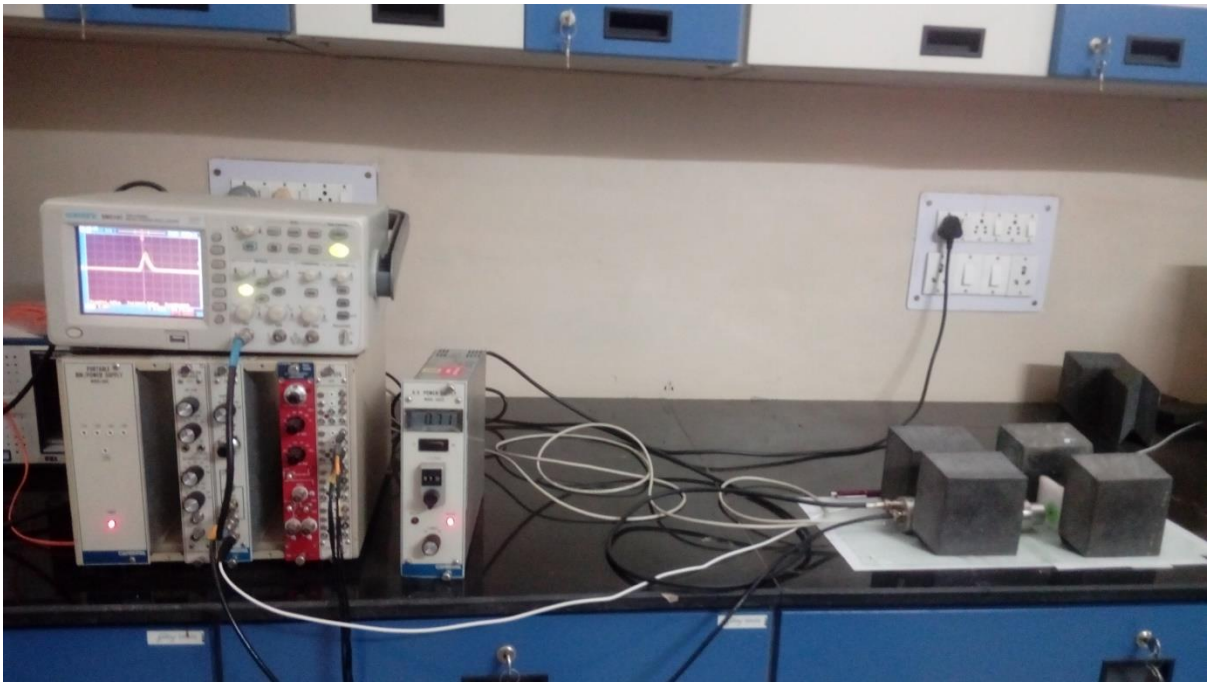

Figure 4.1 Experimental setup for efficiency and resolution measurement

Figure 4.2 Experimental set up for timing measurements

4.1 Scintillator detector:

Experiments are done with the following scintillator

Table 4.1 $LaCl_3$ detector specifications

Crystal type	Crystal size	Model No.	Doping	Operating voltage(kV)
$LaCl_3$:Ce	1″ × 1 ″	Scionix Holland 25.4B25.4/1.5ME2-LAC	0.9%Ce	0.710

Figure 4.3: $LaCl_3$:0.9%Ce scintillation detector with operating voltage 0.710kV

4.2 Preamplifier : Preamplifier is used to avoid changes that can occur to the time constant of a pulse if the PMT is directly connected to the main/linear amplifier.it is generally attach close to the detector to maximize signal to noise ratio.

4.3 Linear amplifier and CRO: It amplifies the signal produced by scintillation detector so that it can be detected by MCA card. It also shape the pulse tail coming from preamp into a linear pulse. Canberra model no. 2022 amplifier and for high voltage supply Canberra model 3002D is used. CRO is used to view the pulses from the linear amplifier.

Figure 4.4 Linear amplifier

4.4 Constant fraction discriminator (CFD): It is used to improve timing performance of the experimental setup. Canberra model 454 is used.

4.5 Delay unit: It is used to introduce a delay in pulse of up to 100ns.

4.6 Time to amplitude converter (TAC): TAC works in conjunction with MCA for energy to timing conversion. It converts the duration of received pulse to into a new pulse of proportional amplitude after that it is analysed by multi-channel analyser (MCA). So each cannel on MCA now represents a time interval. Canberra model 2745 is used for performing timing measurements.

Figure 4.5 CFD

Figure 4.6 TAC

4.7 MCA card

It uses analog to digital convertor (ADC) which converts analog signal produced by scintillator to digital signal. In this experiment a FAST ComTec MCA-3 Series/P7882 PCI express MCA card is used.

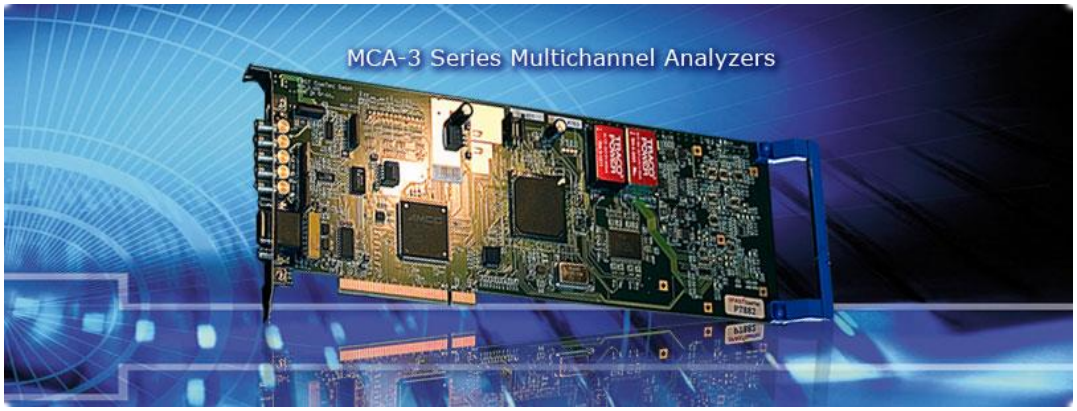

Figure 4.7 PCI-express MCA card installed inside PC

4.8 MCA software

It is used to record and analyse the spectrum on computer. MCA software MCDWIN version 3.13 copyrighted by FAST ComTec is used.

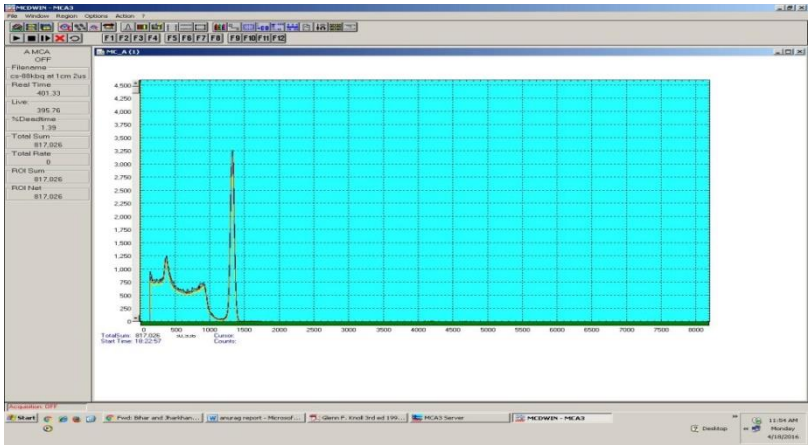

Figure 4.8 Software interface showing energy spectrum for Cs-137

4.9 Gamma sources

Table 4.2 Gamma sources specifications

Source	Activity(kBq)	Manufacturing Date	Half-life(years)
Cs-137	148	June 2002	30
Zn-65	731	March 2013	0.67
Co-60	166.5	June 2002	5.26
Na-22	174	March 2013	2.26
Ba-133	195	March 2013	10.51

Figure 4.9 Different radioactive gamma sources

Chapter 5

Observations

5.1 Energy calibration of $LaCl_3$:Ce

In energy calibration, we express energy as a function of the channel numbers. By finding that relation we can convert channel numbers into their corresponding energies. Energy calibration is done by two gamma sources Cs-137 and Co-60 having energies at 662keV, 1173keV and 1332keV. A graph is plotted between peak channel number and corresponding energies. From the linear fit of this graph we have obtained a relation between energies and corresponding channel numbers.

Table 5.1 ***Measurement for the calibration of $LaCl_3$:Ce scintillation detector by the point sources Co-60 and Cs-137***

S.no.	Peak Channel no.	Peak Energy(keV)
1	1514	662
2	2742	1173
3	3127	1332

5.1.1 Calibration plot

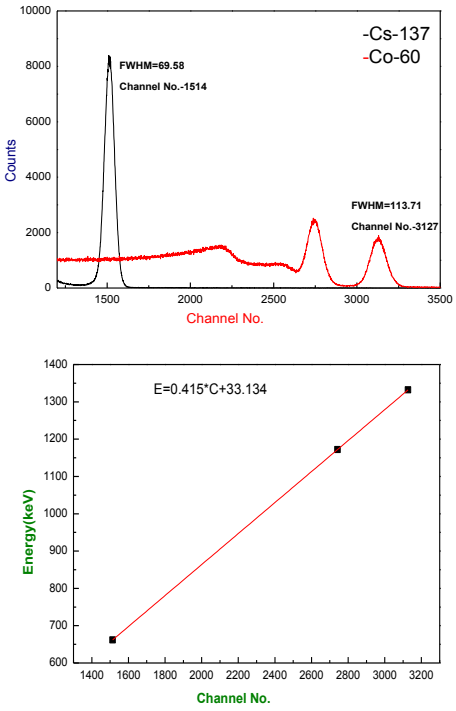

Figure 5.1 Energy calibration Plot using table 5.1

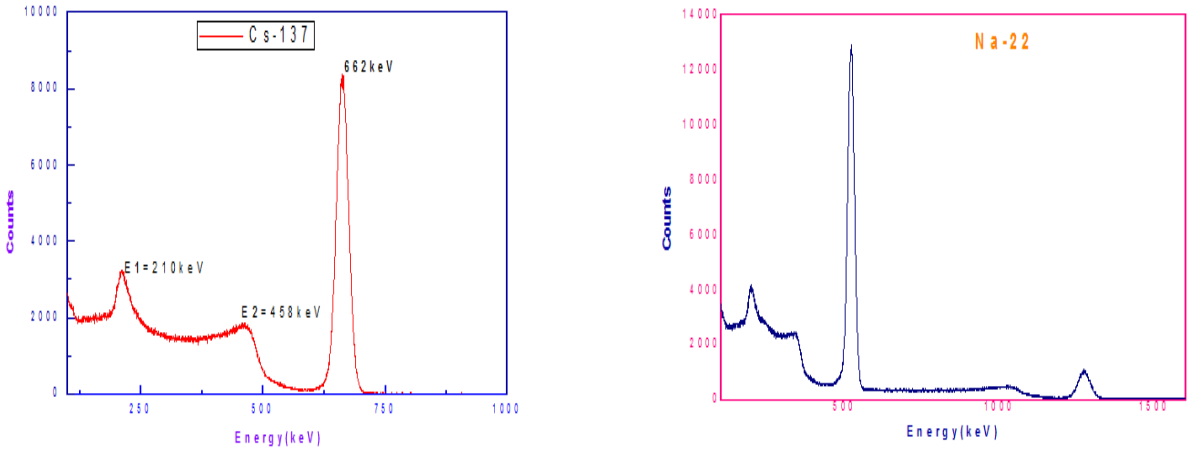

Figure 5.2 Energy spectrum for Cs-137 and Na-22

5.2 Energy Spectra of different sources for different values of source to detector distance

5.2.1 Cs-137

Table 5.2 ***Measurement of peak count rates and total counts under spectrum for Cs-137***

S.No	Distance (cm)	Time(sec)	Counts under photo-peak	Photo peak Count Rate	Total Count Rate
1	0	2011	554667	1849	9435
2	1	1200	1054320	879	4704
3	2	1200	534364	445	2439
4	3	1200	328361	274	1533
5	4	1200	220578	184	1052
6	5	1200	156156	131	773
7	6	1200	121311	101	607
8	7	1200	88557	74	460
9	8	1200	71124	60	373
10	9	1200	59556	52	317
11	10	1790	75142	42	267

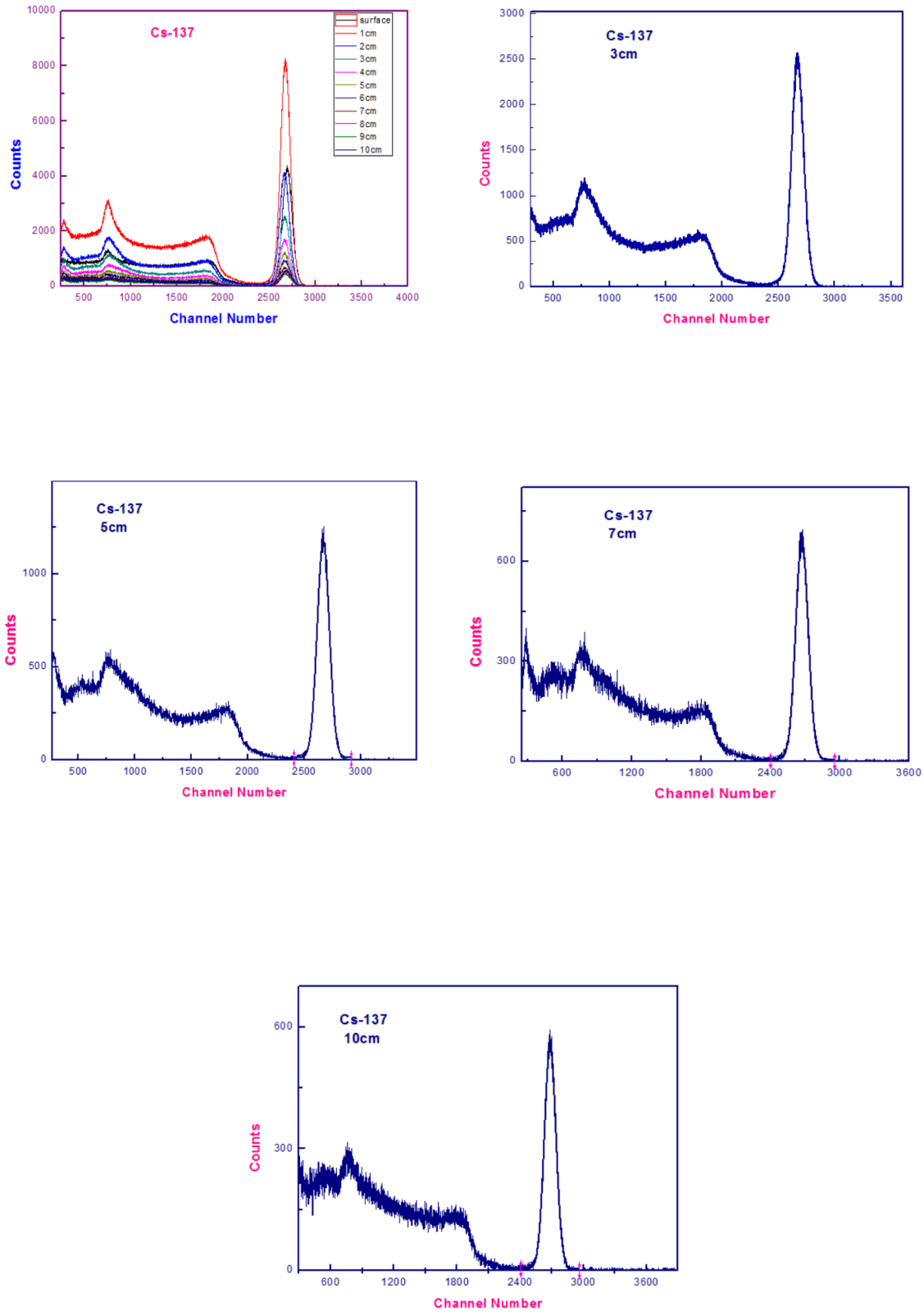

Figure 5.3 Energy spectra for Cs-137 for different values of source to detector distance

5.2.2 Zn-65

Table 5.3 ***Measurement of peak count rates and total counts under spectrum for Zn-65***

S.No	Distance(cm)	Time(sec)	Photo peak count rate	Total count rate
1	0	1992	139	956
2	0.5	1702	91	648
3	1	1631	56	413
4	2	3655	28	235
5	3	1256	12	104
6	4	3200	8	72
7	5	4000	6	52
8	6	4000	4	40

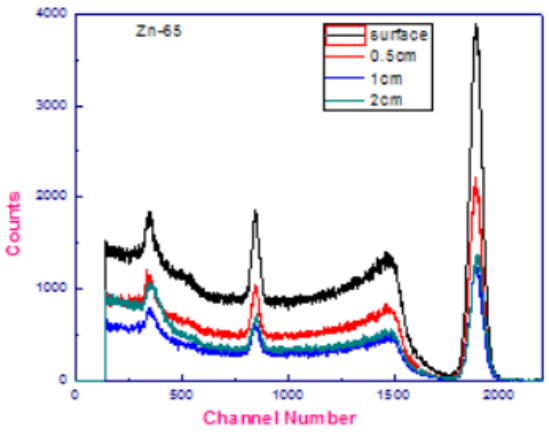

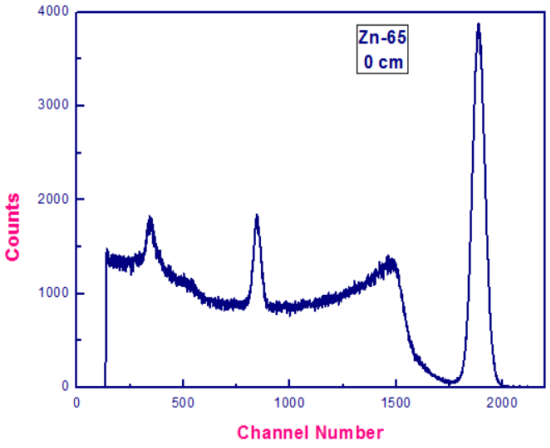

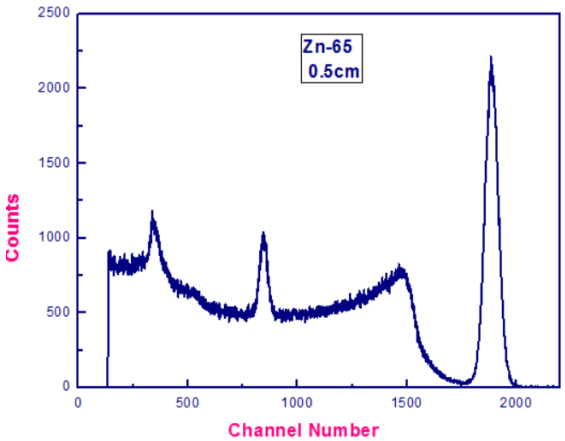

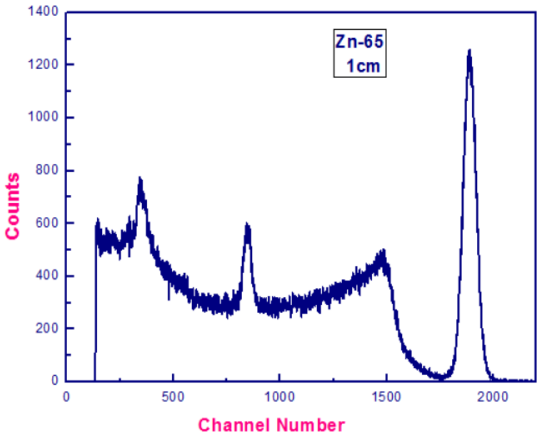

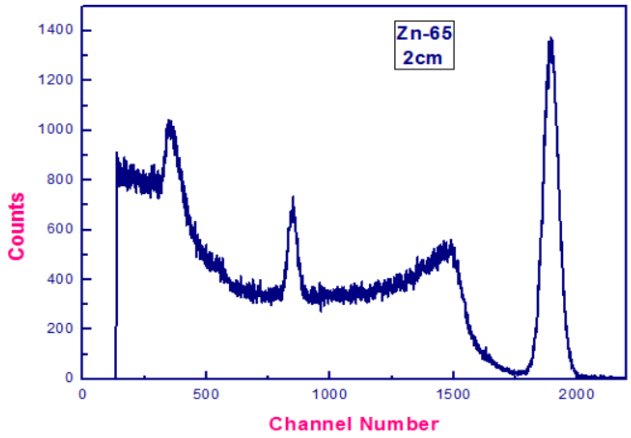

Figure 5.4 Energy spectra for Zn-65 for different values of source to detector distance

5.2.3 Co-60

Table 5.4 ***Measurement of peak count rates and sum peak count rate for Co-60***

Distance (cm)	Count rate for 1_{st} peak (N_1)	Count rate for 2_{nd} peak (N_2)	Count rate for sum peak (N_{12})	Total Count rate (N_t)
0.0	6044	4754	60	60311
0.5	4443	3304	31	41968
1.0	3018	2164	14	28782
1.5	2056	1486	6	19944

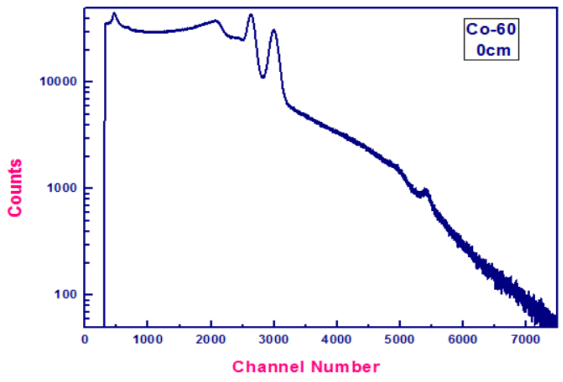

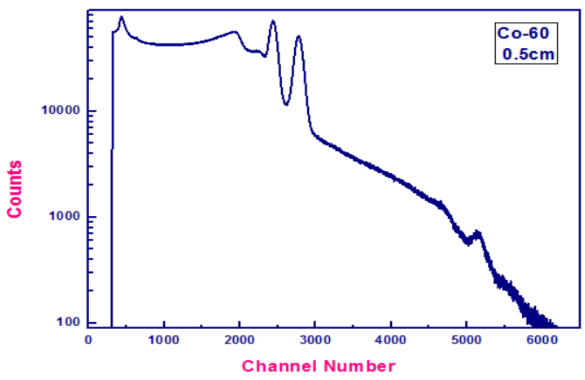

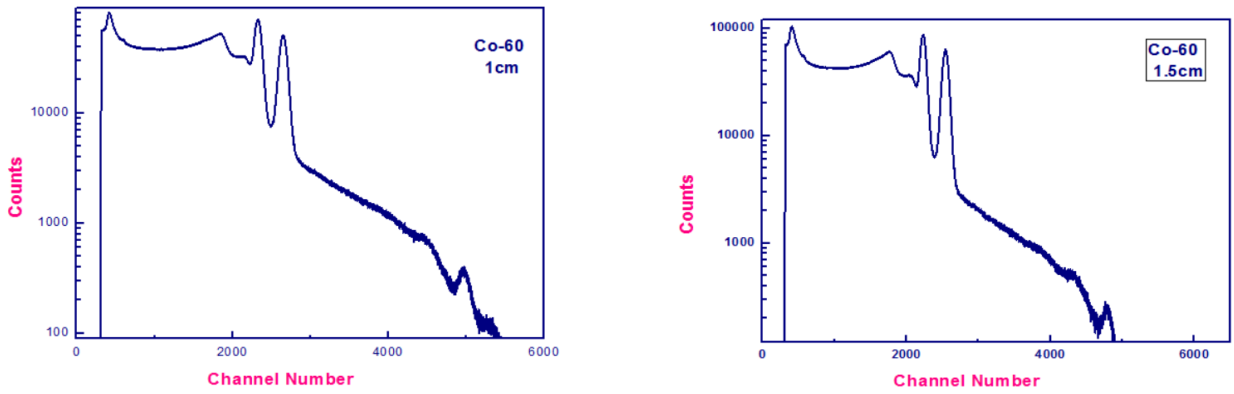

Figure 5.5 Energy spectra for Co-60 for different values of source to detector distance

5.2.4 Na-22

Table 5.5 ***Measurement of peak count rates and sum peak count rate for Na-22***

Distance (cm)	Count rate for 511keV	Count rate for 1275keV	Count rate for sum peak	Total count rate (N_t)
0.0	3986	500	36	17804
0.5	2808	374	18	12299
1.0	1816	250	7	8224
1.5	1533	212	5	5147
2.0	1024	144	2	4586

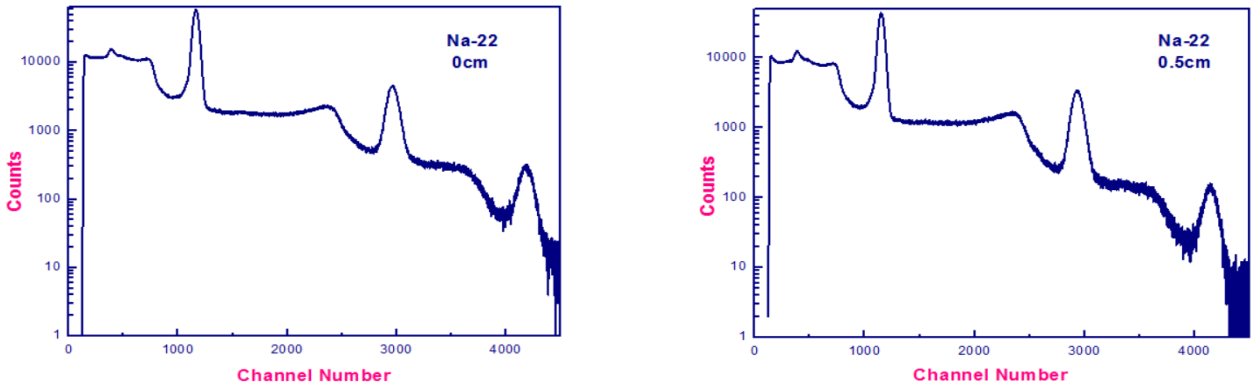

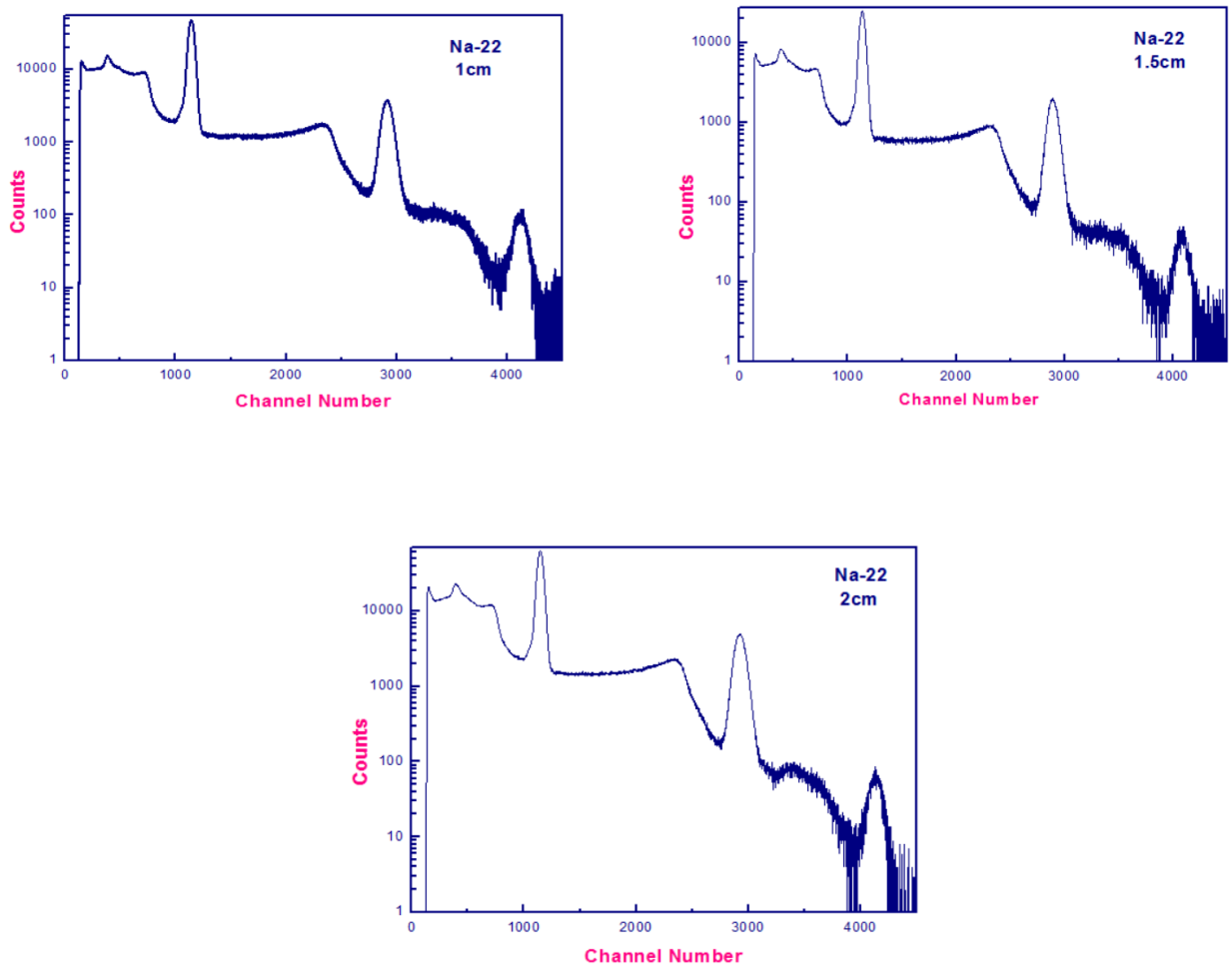

Figure 5.6 Energy spectra for Na-22 for different values of source to detector distance

Chapter 6

Results and Discussion

6.1 Energy resolution at different distances

Table 6.1 ***Energy resolution of $LaCl_3$:Ce for different energies***

S.No.	Distance(cm)	Resolution (%)				
		511keV	662keV	1117keV	1275keV	1332keV
1	0	5.31	4.58(0.14)	3.67(0.18)	3.71(0.13)	3.49(0.15)
2	0.5	5.28	4.60(0.17)	3.69(0.17)	3.66(0.14)	3.53(0.13)
3	1	5.23	4.62(0.19)	3.74(0.14)	3.62(0.12)	3.52(0.14)
4	1.5	5.19	4.60(0.16)	3,73(0.13)	3.64(0.12)	3.57(0.17)
5	2	5.21	4.61(0.12)	3.79(0.12)	3.61(0.11)	3.54(0.11)

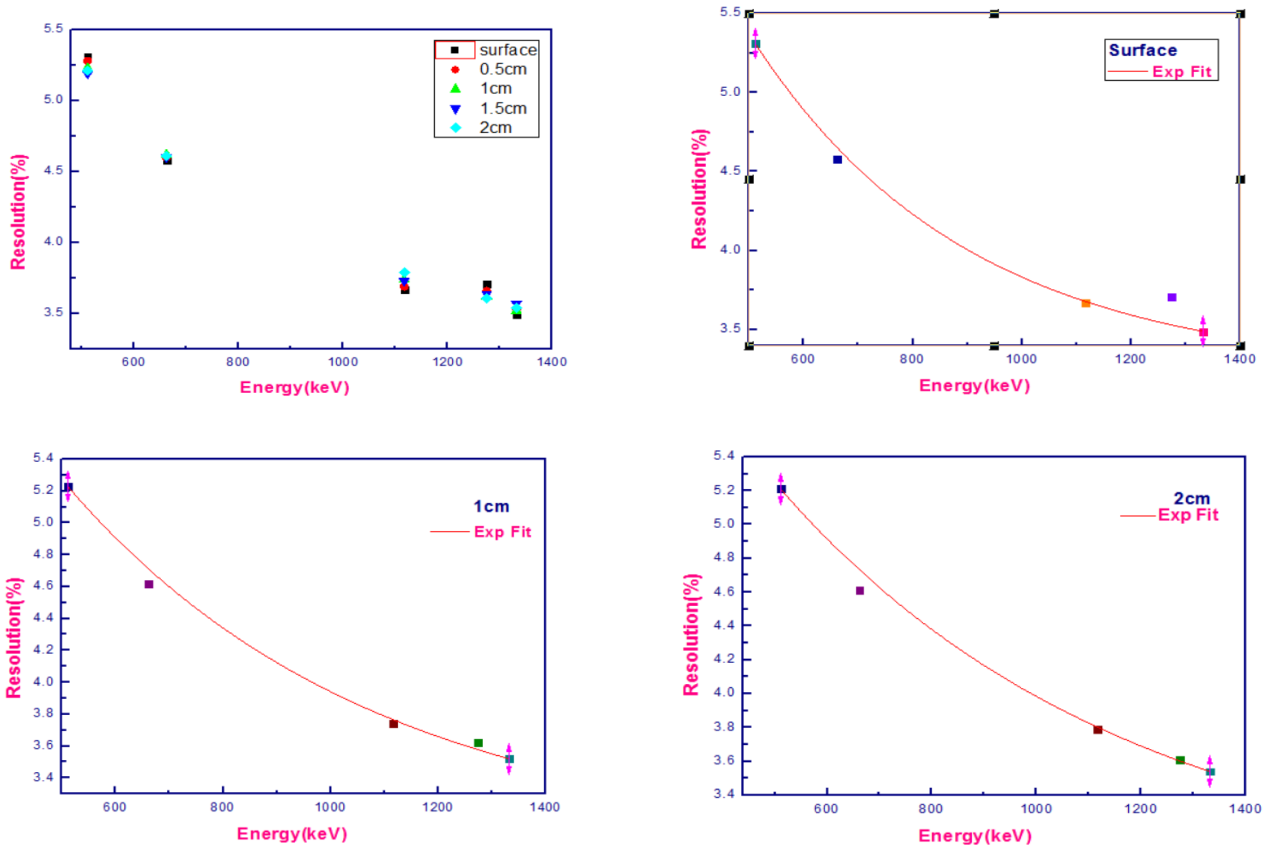

Figure 6.1 Resolution vs gamma energy for different values of source to detector separation.

An energy resolution of 4.58± 0.14% (FWHM) is obtained for 662keV which is in agreement with value quoted by supplier. Energy resolution becomes better as gamma energy increases. This is due to increase in light output with energy.

6.2 Timing resolution: Time resolution of 1.434ns is obtained with two $LaCl_3$ detectors for TAC range 100ns and delay 50ns operating in coincidence with 511keV gamma rays from Na-22 source.

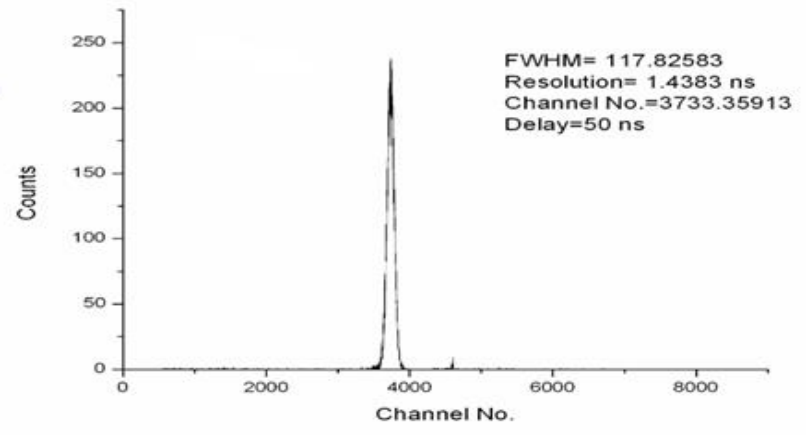

Figure 6.2 Timing spectra by two $LaCl_3$:Ce operating in coincidence with two 511 photons by energy gating.

6.2.1 Speed of light: Speed of light is obtained after measuring timing resolution and it comes out to be 323 275 862 m/s. It is calculated by measuring the slope of following graph

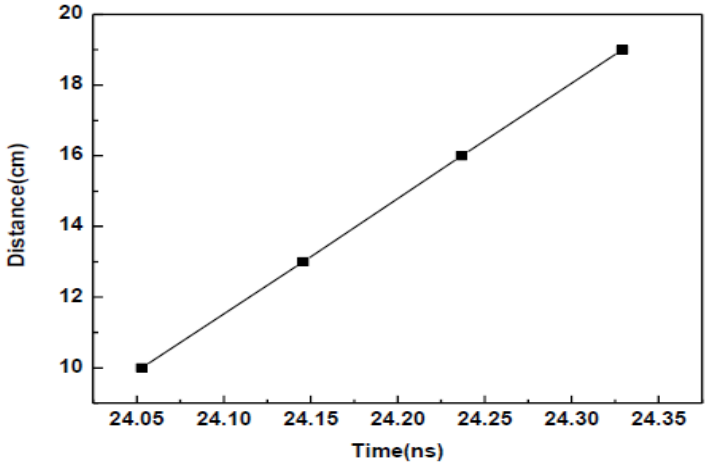

Figure 6.3 Distance vs time graph for $LaCl_3$:Ce

6.3 Efficiencies

6.3.1 For single gamma emitters

6.3.1.1 Cs-137

Table 6.2 ***Absolute photo-peak and absolute total detection efficiency at different distances for Cs-137***

S. No	Distance (cm)	Absolute photo- peak efficiency (%)	Absolute total detection efficiency (%)
1	0	2.02(0.047)	10.285(0.017)
2	1	0.958(0.032)	5.132(0.019)
3	2	0 .488(0.045)	2.658(0.021)
4	3	0.300(0.018)	1.671(0.021)
5	4	0.201(0.014)	1.14(0.027)
6	5	0.142(0.012)	0.842(0.030)
7	6	0.110((0.011)	0.661(0.035)
8	7	0.081(0.009)	0.501(0.043)
9	8	0.065(.008)	0.406(0.054)
10	9	0.056(0.008)	0.345(0.077)
11	10	0.045(0.006)	0.291(0.111)

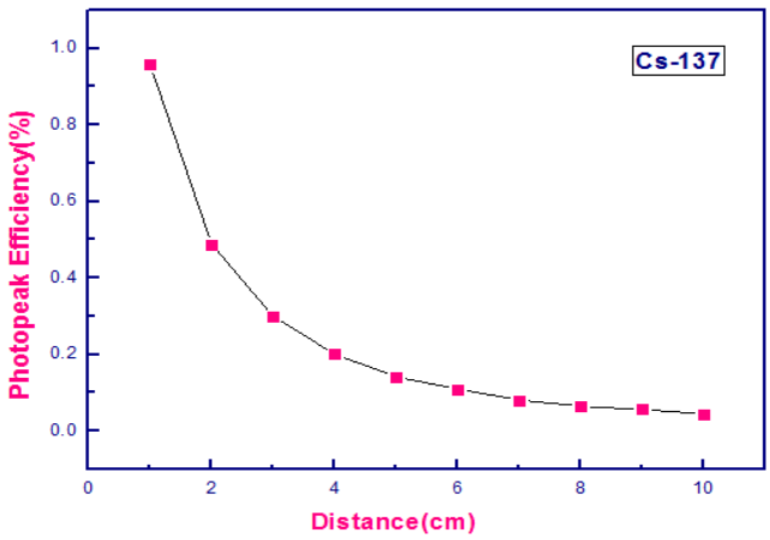

Figure 6.4 Variation of absolute photo-peak efficiency of $LaCl_3$:Ce with different values of source to detector distances for 662keV gamma(Cs-137)

6.3.1.2 Zn-65

Table 6.3 ***Absolute photo-peak and absolute total detection efficiency at different distances for Zn-65***

S.No.	Distance(cm)	Abs. photo-peak efficiency (%)	Abs. total detection efficiency (%)
1	0	0.643(0.055)	4.524(0.147)
2	0.5	0.425(0.045)	3.066(0.121)
3	1	0.265(0.035)	1.954(0.096)
4	2	0.133(0.025)	1.112(0.072)
5	3	0.0791(0.023)	0.685(0.067)
6	4	0.0527(0.019)	0.474(0.055)
7	5	0.0362(0.015)	0.342(0.047)
8	6	0.0263(0.013)	0.263(0.041)

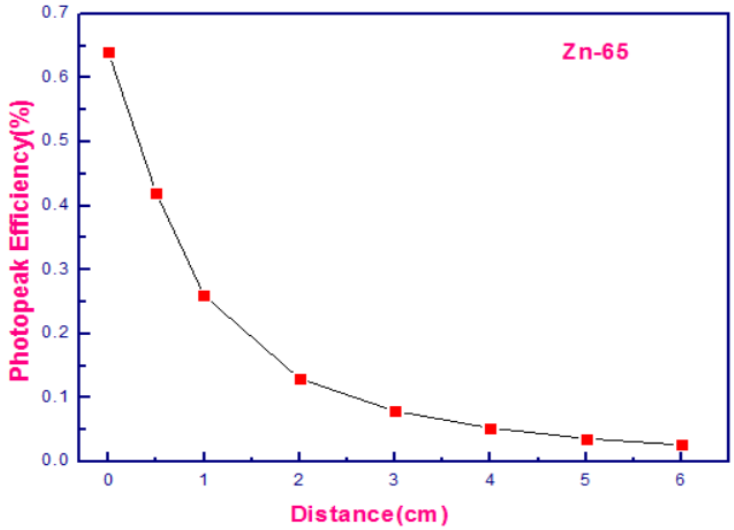

Figure 6.5 Variation of absolute photo-peak efficiency of $LaCl_3$:Ce with different values of source to detector distances for 1120keV gamma (Zn-65).

Here we can see that photo-peak efficiency is decreasing as source to detector distance is increasing. It decreases with distance because of decrease in photo-peak counts with distance as solid angle decreases with distance.

6.3.2 Double gamma emitters

6.3.2.1 Co-60

Table 6.4 ***Absolute photo-peak and absolute total detection efficiency at different values of source to detector distance for Co-60***

Distance (in cm)	**Peak Efficiency (ε_1) at Energy 1173keV (%)**	**Peak Efficiency (ε_2) at Energy 1332keV (%)**	**Total Efficiency (η_1) at Energy 1173keV (%)**	**Total Efficiency (η_2) at Energy 1332keV (%)**
0	1.17(0.001)	0.917(0.001)	8.4(0.12)	7.6(0.12)
0.5	0.85(0.002)	0.64(0.001)	9.1(0.22)	7.9(0.22)
1	0.58(0.003)	0.42(0.002)	9.9(0.48)	8.5(0.49)
1.5	0.381(0.004)	0.277(0.003)	5.5(1.18)	4.79(1.19)

6.3.2.2 Na-22

Table 6.5 ***Absolute photo-peak and absolute total detection efficiency at different values of source to detector distance for Na-22***

Distance (cm)	**Measured peak efficiency at 511keV (%)**	**Measured peak efficiency at 1275keV (%)**	**Measured total detection efficiency at 511keV (%)**	**Measured total detection efficiency at 1275keV (%)**
0	3.12(1.7)	0.836(1.7)	12.17(0.14)	7.40(0.22)
0.5	2.17(1.2)	0.600(1.2)	10.36(0.12)	6.31(0.19)
1	1.37(1.38)	0.370(1.38)	6.57(0.21)	3.91(0.35)
1.5	1.15(1.11)	0.313(1.11)	6.49(0.17)	3.86(0.28)
2	0.749(1.06)	0.193(1.06)	1.56(0.68)	0.903(1.17)

6.4 Photo-fraction

6.4.1 Cs-137

Table 6.6 ***Measured photo-fraction of $LaCl_3$:Ce for Cs-137 at different source to detector distance***

S.No.	Distance(cm)	Photo fraction
1	0	0.195(0.004)
2	1	0.186(0.006)
3	2	0.182(0.009)
4	3	0.178(0.011)
5	4	0.174(0.013)
6	5	0.179(0.016)
7	6	0.166(0.017)
8	7	0.160(0.022)
9	8	0.160(0.022)
10	9	0.164(0.024)
11	10	0.157(0.004)

The reported photo fraction is in good agreement with the value quoted by M. Balcerzyk *et al*. [7].

6.4.2 Zn-65

Table 6.7 ***Measured photo-fraction of $LaCl_3$:Ce for Zn-65 at different source to detector distance***

S.No.	Distance(cm)	Photo fraction
1	0	0.145(0.013)
2	0.5	0.140(0.015)
3	1	0.135(0.019)
4	2	0.119(0.023)
5	3	0.115(0.035)
6	4	0.111(0.041)
7	5	0.105(0.045)
8	6	0.100(0.052)

6.5 Simulations

For verifying the validity of my results, we have compared my results with simulated results. For simulation, we have used the GEANT4 simulation toolkit which simulates the passage of particles through matter. It is developed by CERN with the help of collaborators from software engineers and particle physicists. It uses the object oriented C++ programming language. Its applications include nuclear physics, medical physics, particle physics, space engineering, etc.

6.5.1 Cs-137

Table 6.8 ***Measured and simulated values of photo-peak efficiencies for Cs-137 at different source to detector distance***

S. No.	Distance(cm)	Measured photo-peak efficiency (%)	Simulated photo-peak efficiency (%)
1	1	0.958	1.08
2	2	0 .488	0.54
3	3	0.300	0.32
4	4	0.201	0.22
5	5	0.142	0.159
6	6	0.110	0.115
7	7	0.081	0.087
8	8	0.065	0.067
9	9	0.056	0.054
10	10	0.045	0.046

6.5.2 Co-60

Table 6.9 ***Measured and simulated values of photo-peak efficiencies for Co-60 at different source to detector distance***

Distance (in cm)	Measured peak efficiency at 1173keV (%)	Simulated efficiency at 1173keV (%)	Measured peak efficiency at 1332keV (%)	Simulated efficiency at 1332keV (%)
0	1.15	1.33	0.917	0.925
0.5	0.85	0.736	0.64	0.626
1	0.58	0.463	0.42	0.392
1.5	0.381	0.321	0.277	0.270

6.5.3 Na-22

Table 6.10 ***Measured and simulated values of photo-peak efficiencies for Na-22 at different source to detector distance***

Distance (in cm)	Measured peak efficiency at 511keV (%)	Simulated efficiency at 511keV (%)	Measured peak efficiency at 1275keV (%)	Simulated efficiency at 1275keV (%)
0	3.12	4.73	0.836	1.19
0.5	2.17	2.64	0.600	0.65
1	1.37	1.65	0.370	0.42
1.5	1.15	1.12	0.313	0.29
2	0.749	0.82	0.193	0.21

Table 6.11 ***Measured and simulated values of total detection efficiencies for Na-22 at different source to detector distance***

Distance (cm)	Measured total detection efficiency at 511keV (%)	Simulated efficiency at 511keV (%)	Measured total detection efficiency at 1275keV (%)	Simulated efficiency at 1275keV (%)
0	12.17	11.81	7.40	7.70
0.5	10.36	6.51	6.31	4.24
1	6.57	4.12	4.00	2.66
1.5	6.49	2.77	3.86	1.81
2	1.56	2.00	0.903	1.31

From the above comparisons we found that measured and simulated results are in good agreement with each other.

Chapter 7

Summary

In the present work, investigations were done with $LaCl_3$:0.9%Ce detector for gamma ray spectroscopy. The measurements have shown that $LaCl_3$:Ce is a very good scintillation detector for γ-ray spectroscopy. It has good energy resolution of $4.58\pm 0.14\%$ (FWHM) for 662keV which is in agreement with value quoted by supplier. Also it is very efficient, has good linear response and good timing resolution (1.43ns). Due to these attractive properties $LaCl_3$:Ce can be used in applications such as nuclear and high energy physics, medical imaging, non-destructive evaluation, X-ray diffraction, treaty verification and safeguards, geological exploration and environmental monitoring.

Publication

K.Thakur,M.Dhibar,G.Anil Kumar et al., *"Close-geometry efficiency calibration of LaCl3:Ce detectors:Measurements and Simulations"*, DAE Symposium on Nuclear Physics (Govt. of India), 60 (2015) 1034.

CHAPTER 8

References

[1] O. Guillot-Noe¨l, *et al*.,J. Lumin. 85(1999) 21.

[2] E.V.D. Van Loef, *et al*.,Appl. Phys. Lett. 77 (2000) 1467.

[3] E.V.D. van Loef, *et al*.,IEEE Trans. Nucl. Sci. NS-48 (2001) 341.

[4] C.P. Allier *et al*.,Nucl. Instru. and Meth.485 (2002) 547.

[5] K.S. Shah *et a*l.,Nucl. Instru. and Meth.505 (2003) 76.

[6] T. Vidmar *et al.*,Nucl. Instru. and Meth.508 (2003) 404.

[7] M. Balcerzyk *et al*.,Nucl. Instru. and Meth.537 (2005) 50–56.

[8] Mohini W.Rawool-Sullivan *et al*.,Elevsier science (2005).

[9] B. Ayaz-Maierhafer,*et al.* ,Nucl. Instru. and Meth.579 (2007) 410.

[10] D. Alexiev *et al*., IEEE Transactions on nuclear science,55(June 2008).

[11] G. Anil Kumar *et al.*,Nucl. Instru. and Meth.609 (2009) 183–186.

[12] J. Andriessen *et al*.,Optics Communications 178 (2000) 355.

[13] A. Owens et al.,Nucl. Instru. and Meth.574 (2007) 110.

[14] W. Drozdowski, P. Dorenbos *et al.* , IEEE Transactions on Nuclear Sciences 54 (2007).

[15] M. Tsutsumi, Y. Tanimura , Nucl. Instru. and Meth. 557 (2006) 554.

[16] R. Novotny, Nucl. Instr. and Meth. 537 (2005) 1.

[17] C. D'Ambrosio *et al.*, Nucl. Instru. and Meth. 556 (2006) 187.

[18] Arnold, D., *et al*., J. Radioanal. Nucl. Chem. 248 (2001) 365.

[19] Semkow, T.M., Mehmood,*et al.*,Nucl. Instrum. Methods 290 (1999) 437.

[20] Andreev, D.S., Erokhina, *et a*l.,Instrum. Exper. Technol.15(1972) 1358.

[21] G. Knoll, Radiation Detection and Measurement, 3rd Edition, Wiley, NewYork, (1999).

[22] P. R. Menge, G. Gautier *et al*., *Nucl. Instrum. Meth.*579 (2007) 6.

[23] T. Kamae *et al.*,Nucl. Instr. and Meth. 490 (2002) 456.